

Cite this article as: Li Jiawen, Liu Sicong, Huang Sirui, et al. Preparation and Mechanical Properties of FeMnCu Medium Entropy Alloy Matrix Composites Reinforced with TiC Particles[J]. Rare Metal Materials and Engineering, 2023, 52(04): 1169-1175.

ARTICLE

Preparation and Mechanical Properties of FeMnCu Medium Entropy Alloy Matrix Composites Reinforced with TiC Particles

Li Jiawen, Liu Sicong, Huang Sirui, Zhu Heguo

College of Materials Science and Engineering, Nanjing University of Science and Technology, Nanjing 210094, China

Abstract: x TiC/FeMnCu($x=2.5, 5, 7.5, 10$, vol%) composites were fabricated by vacuum induction melting and then annealed. X-ray diffraction (XRD), scanning electron microscope (SEM) and energy dispersive spectrum (EDS) were used to analyze the phase constitution and microstructure, and the tensile properties of the samples were investigated by the universal tensile testing machine. The results show that the x TiC/FeMnCu($x=2.5, 5, 7.5, 10$, vol%) composites exhibit a biphasic face-centred cubic structure. With the increase in x value, the matrix structure of the composites is significantly refined and the tensile strength gradually increases, which is due to the combined effect of fine grain strengthening, thermal mismatch strengthening and Orowan strengthening. After 10TiC/FeMnCu is annealed at 600 °C for 4 h and 800 °C for 4 h, the structure does not change significantly, and carbides are precipitated in the matrix. The tensile strength of the sample increases but the elongation decreases slightly.

Key words: medium entropy alloys; vacuum induction melting; TiC reinforcement; mechanical properties

The concept of multi-principal alloys has been proposed decades ago, and researchers have made considerable efforts to further understand this new material, and provided valuable information and experience for future scientific work^[1-2]. The introduction of the multi-principal alloy concept has brought great scope for the development in the field of metallic materials research and has challenged the theoretical limit values of conventional alloys. With the deepening of research, a certain theoretical basis has been established, but there are still problems such as the lack of mature understanding of the whole system and the absence of a systematic and complete theory to support the guidance. In addition, there are still a certain limitation in the performance of medium/high entropy alloys and related composites under some special conditions and the performance cannot be maximized^[3-6], which need to be further explored and researched. At present, the research hotspots for medium/high entropy alloys are mainly the basic alloy theory, the development and design of new alloy systems^[7], the alloy preparation methods and the toughening

methods^[8-10].

As a new type of multi-principal alloy system, ternary medium entropy alloys are easy to form simple solid solutions due to the high entropy effect. The proximity of the atomic size between the main elements makes the lattice atoms uncertain, which leads to lattice distortion and easy solid solution strengthening^[11-13]. Thus the alloy possesses excellent mechanical properties^[14-17] and high research value. However, there is still a lack of understanding for the medium-entropy alloy systems. For example, the mostly studied CrCoNi medium entropy alloy has a single-phase face-centred cubic structure with good fracture toughness and possesses a strength better than most high-entropy alloys^[18-19], and is very susceptible to deformation twinning during plastic deformation and significant work-hardening phenomena^[20-21], but it still has the problem of low yield strength. Therefore, further research is needed^[22-24].

The FeMnCu system alloy, as a new ternary medium entropy alloy, has a molar entropy value of 1.1R lower than

Received date: May 02, 2022

Foundation item: National Natural Science Foundation of China (51571118)

Corresponding author: Zhu Heguo, Ph. D., Professor, College of Materials Science and Engineering, Nanjing University of Science and Technology, Nanjing 210094, P. R. China, E-mail: zhg1200@njjust.edu.cn

Copyright © 2023, Northwest Institute for Nonferrous Metal Research. Published by Science Press. All rights reserved.

that of most conventional multi-principal alloys, while research on its phase composition, microstructure and properties is relatively scarce. At the same time, TiC, as a ceramic particle, is often introduced into the alloy system as a second phase reinforcing particle to form a composite material to enhance the properties of the alloy^[25-27]. Therefore, this study investigated the preparation and mechanical properties of FeMnCu medium entropy alloy matrix composites reinforced with TiC particles, and the annealing heat treatment process of the composites.

1 Experiment

FeMnCu medium entropy alloy matrix composites reinforced with TiC particles, x TiC/FeMnCu ($x=2.5, 5, 7.5, 10, \text{vol}\%$) were prepared using iron powder (purity 99.8%, 30–50 μm in diameter), titanium powder (purity 99.8%, 30–50 μm in diameter), carbon powder (purity 99.9%, 1–5 μm in diameter), iron particles, manganese particles and copper particles as reaction materials. The mass of each component element required to prepare 40 g TiC-reinforced medium entropy alloy based composites with different volume fractions of TiC was calculated. The titanium powder, carbon powder and iron powder were mixed and ball-milled for 8 h and then pressed into cylindrical specimens with 20 mm in diameter and 2–4 mm in height. The weighed iron particles, manganese and copper blocks were put into corundum crucibles together with the cylindrical specimens and melted in a vacuum induction melting furnace. A mechanical pump and a molecular pump were used to evacuate the vacuum to 10^{-3} Pa, and the temperature was slowly increased at a rate of 30 °C/min until the metal particles in the corundum crucible were completely melted, and the molten alloy liquid was poured into the copper crucible in the melting furnace after a period of heat preservation. The 10TiC/FeMnCu composite was annealed at 600 °C for 4 h and 800 °C for 4 h.

The specimens were wire cut as well as ground and polished. The microstructure was investigated by scanning electron microscopy (SEM), energy spectroscopy (EDS) and X-ray diffraction (XRD). The room temperature tensile properties were tested by a universal tensile tester, and the fractures were scanned and observed.

2 Results and Discussion

2.1 XRD analysis

The XRD patterns of the x TiC/FeMnCu ($x=2.5, 5, 7.5, 10, \text{vol}\%$) composites are shown in Fig. 1. It can be seen that the FeMnCu medium entropy alloy matrix exhibits a biphasic face-centred cubic (fcc) structure. The doping of TiC particles does not change the phase structure of the master alloy and x TiC/FeMnCu ($x=2.5, 5, 7.5, 10, \text{vol}\%$) composites still exhibit a biphasic structure. The diffraction peaks of TiC appear at 41° and 61°, which gradually become more pronounced with increasing x values. Compared to the FeMnCu alloy matrix, the diffraction peaks of the x TiC/FeMnCu(x =

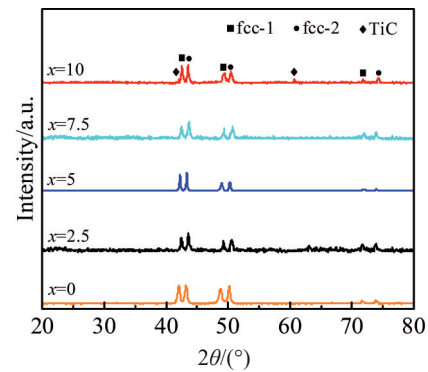


Fig.1 XRD patterns of x TiC/FeMnCu ($x=2.5, 5, 7.5, 10, \text{vol}\%$) composites

2.5, 5, 7.5, 10, vol%) alloys are slightly shifted to the right and mostly pronounced at $x=10$, which can be explained by the distortion of the lattice with the incorporation of TiC ceramic particles into the system, which intensifies the lattice distortion and in turn leads to a change in the grain plane spacing.

2.2 SEM analysis

The SEM and EDS results of the x TiC/FeMnCu composites are shown in Fig. 2. The surface morphology clearly shows that the FeMnCu alloy matrix consists of dark grey Cu-poor areas together with light grey Cu-rich areas, and the microstructure of alloy with TiC particles is significantly finer and denser than that without particles. From the EDS spectrum in Fig. 2f, it can be seen that the matrix is embedded with black TiC-enhanced particles with different sizes and in a polymorphic pattern, and the TiC particles are randomly distributed with significant interdendritic bias of Cu elements, which may be a sign that TiC completely wets the grain boundaries^[28-29]. From Fig. 2a–2e, it can be seen that the TiC-enhanced particles are uniformly distributed in the FeMnCu alloy matrix, while with the increase in TiC content, the TiC particles in the system increase and the distribution of TiC particles in the matrix undergoes agglomeration, which is the most obvious when the TiC content is 10vol%.

Fig. 3 shows the size distribution of TiC particles in the x TiC/FeMnCu ($x=2.5, 5, 7.5, 10, \text{vol}\%$) composites; as the TiC content in the system increases, the particles of the reinforcing phase are refined and the average particle size is 1.07, 1.01, 0.67 and 0.68 μm in that order. The surface scan image of 10TiC/FeMnCu was analyzed in order to determine the distribution of elements in the composite system. As shown in Fig. 4, the Mn element is uniformly dispersed in the composite matrix, while the Fe and Cu elements are mainly distributed in different matrix regions, which corroborates the XRD and SEM characterization results. In particular, C element is dispersed in the matrix, with the presence of some slightly brighter positions, indicating a higher concentration of C element. The irregular polygonal bright spots containing Ti are also observed, indicating that TiC reinforced phase is randomly distributed in the matrix.

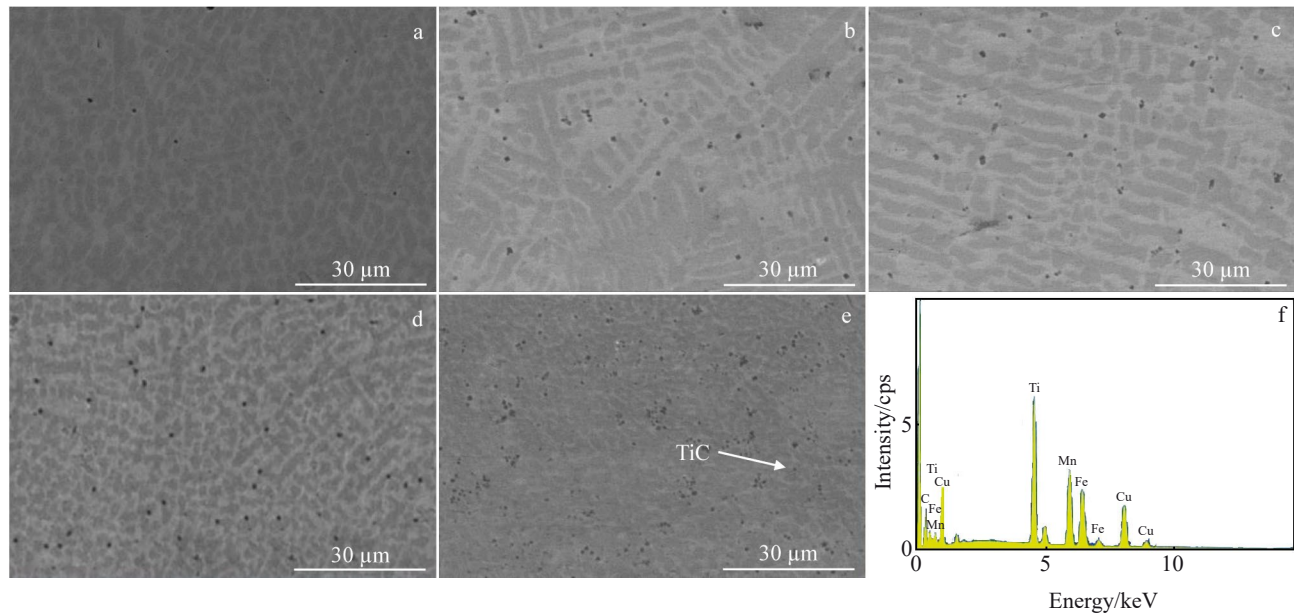


Fig.2 SEM images (a–e) and EDS spectrum (f) of x TiC/FeMnCu ($x=2.5, 5, 7.5, 10$, vol%) composites: (a) matrix, (b) $x=2.5$, (c) $x=5$, (d) $x=7.5$, and (e) $x=10$

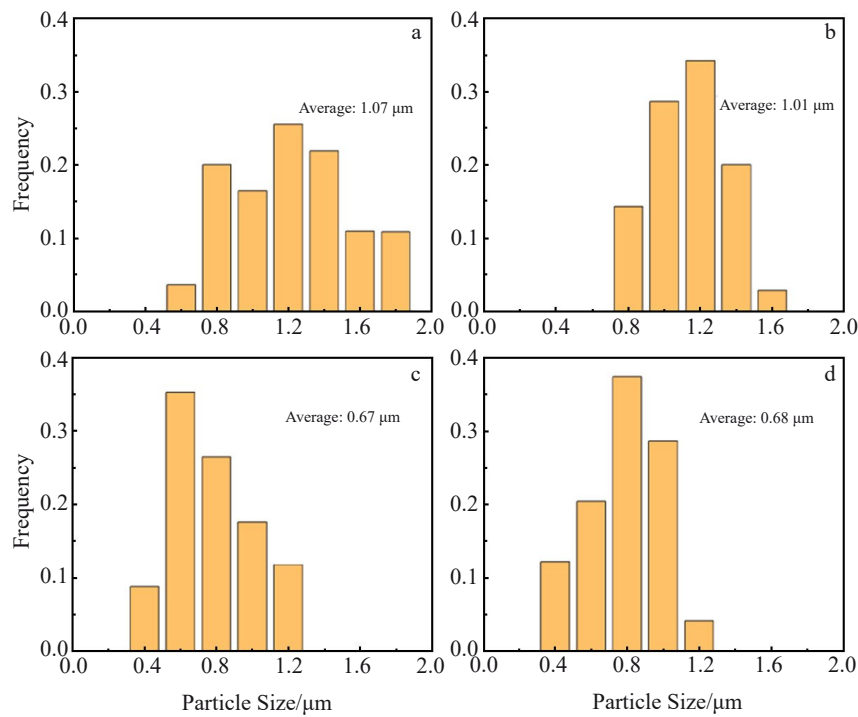


Fig.3 TiC particle size distribution in x TiC/FeMnCu ($x=2.5, 5, 7.5, 10$, vol%) composites: (a) $x=2.5$, (b) $x=5$, (c) $x=7.5$, and (d) $x=10$

2.3 Analysis of tensile properties

The tensile stress-strain curves for the x TiC/FeMnCu ($x=2.5, 5, 7.5, 10$, vol%) composites are shown in Fig. 5. It can be seen that the incorporation of TiC reinforcing particles has a strengthening effect on the FeMnCu alloy. The tensile strength and elongation at break of the composites increase compared

to those of the FeMnCu alloys. As the volume fraction of TiC increases to 2.5vol% , 5vol% , 7.5vol% , and 10vol% , the tensile strength of the composites increases gradually to 594, 607, 633 and 648 MPa, respectively, while the elongation at break shows an increasing trend followed by a decreasing trend to 43.9%, 42.4%, 39.8% and 32.4%, respectively. The

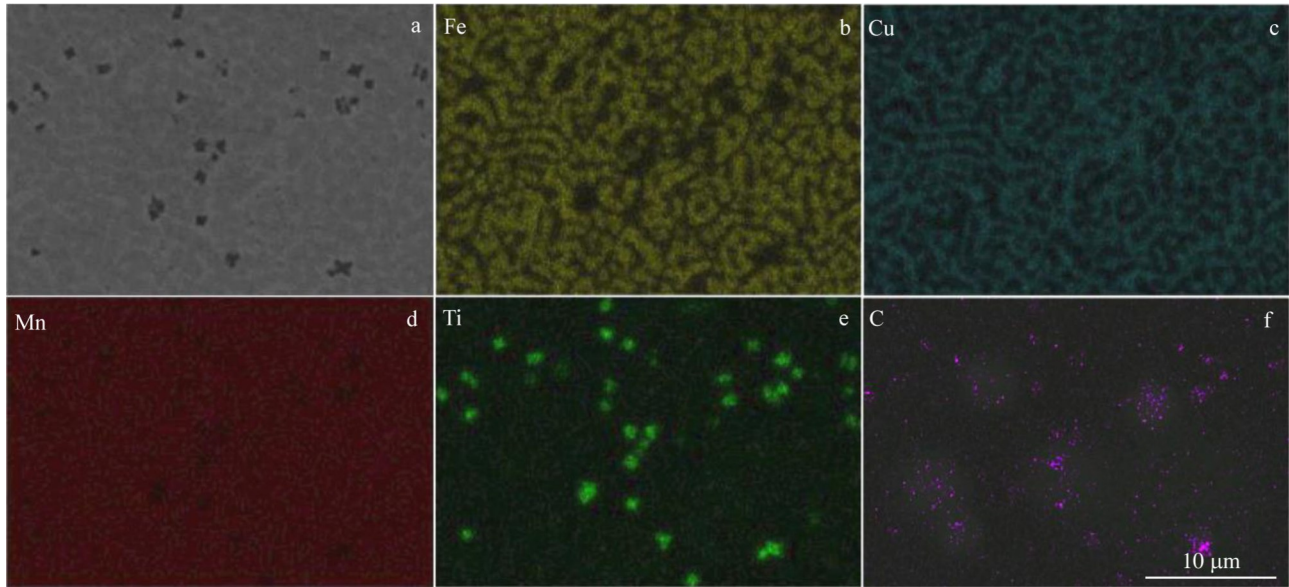


Fig.4 SEM image (a) and EDS mappings of element Fe (b), Cu (c), Mn (d), Ti (e), and C (f) of 10TiC/FeMnCu composites

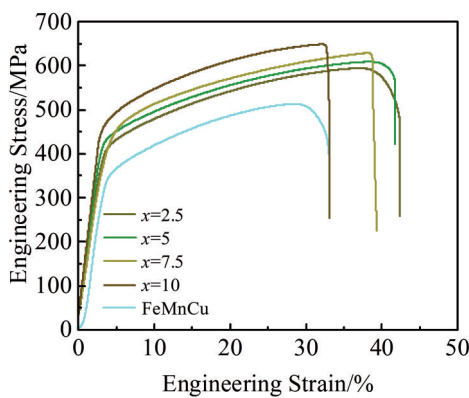


Fig.5 Stress-strain curves for x TiC/FeMnCu ($x=2.5, 5, 7.5, 10$, vol%) composites

highest tensile strength is achieved when the content of TiC is 10vol%, increased by 138 MPa compared to that of FeMnCu alloy, and the highest elongation is achieved when the content of TiC is 2.5vol%, increased by 135% compared to that of FeMnCu alloy.

The main strengthening mechanisms in the x TiC/FeMnCu ($x=2.5, 5, 7.5, 10$, vol%) composites are fine grain strengthening, thermal mismatch strengthening and Orowan strengthening. Due to the large size of the TiC particles, there is a strong impediment to grain boundary movement, resulting in a finer structure and greater resistance to dislocation migration, which in turn increases the strength of the composite. According to the Hall-Petch relationship, the smaller the grain size, the more obvious the strengthening effect, and the strengthening effect is significant when the TiC content is 10vol%. At the same time, the difference between the thermal expansion coefficients of TiC particles and

FeMnCu matrix will lead to different degrees of thermal deformation of the matrix and reinforcing phase when the temperature of the composite changes, resulting in residual stresses caused by thermal mismatch at the contact between the matrix and reinforcing phase, and causing plastic deformation of the alloy matrix near the interface. And the dislocation density increases at this location, increasing the resistance for dislocation to slip, and thus increasing the strength of the composites. In addition, TiC second phase reinforced particles form in the alloy matrix, which are uniformly and randomly distributed. The dislocation movement is impeded by the hard reinforcing particles, leaving a dislocation ring when the dislocation passes through the reinforcing phase, and the dislocation ring acts as a reverse force to further increase the resistance to dislocation slip, thus increasing the strength of the composites. The critical shear stress of dislocation line movement in the composites is directly related to the volume fraction of the reinforcing phase and the radius of the reinforcing phase particles. Therefore, there is a significant dispersion strengthening effect when the TiC content in the system is higher and the average particle size is less than 1 μm .

The tensile fractures of the x TiC/FeMnCu ($x=0, 2.5, 5, 7.5, 10$, vol%) composites were analyzed by SEM and the results are shown in Fig. 6. From the surface morphology of the fractures of the FeMnCu matrix and x TiC/FeMnCu ($x=2.5, 5, 7.5, 10$, vol%) composites, it can be observed that the necking phenomenon occurs in all specimens and disappears with increasing TiC content. The tensile fractures of the specimens are clustered with many dimples with different sizes, all of which are typical of ductile fractures. As the TiC content increases, the dimples become smaller and the fracture is denser. At the same time, better tensile properties can be explained in a certain extent by the larger and deeper

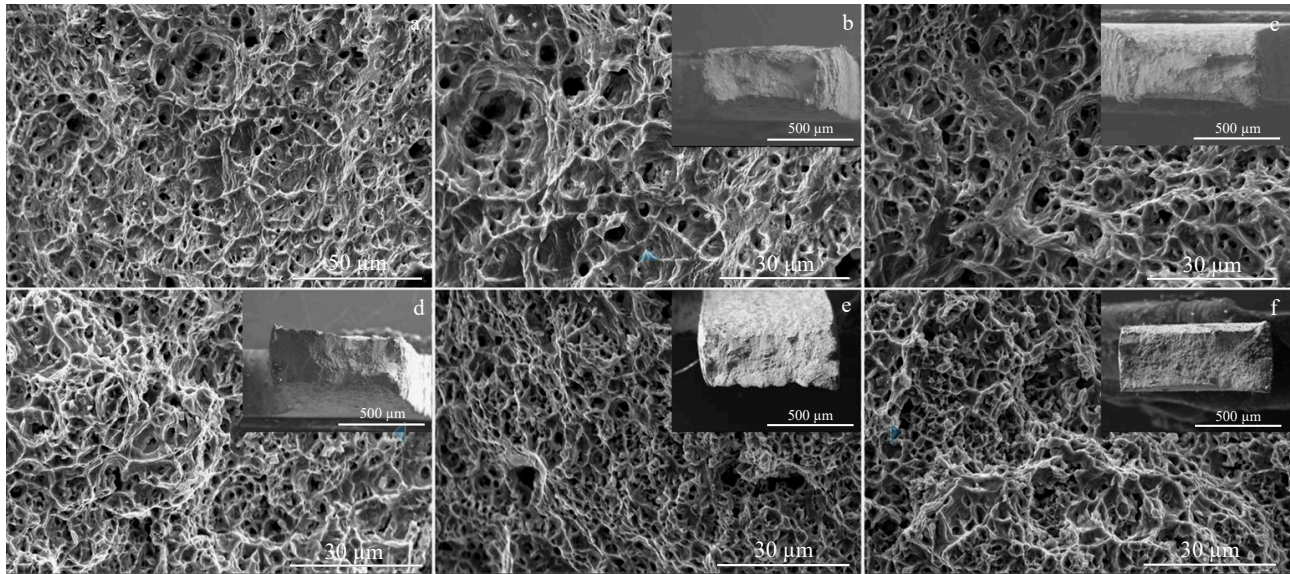


Fig.6 Fracture morphologies of x TiC/FeMnCu ($x=0, 2.5, 5, 7.5, 10, \text{vol}\%$) composites: (a, b) matrix, (c) $x=2.5$, (d) $x=5$, (e) $x=7.5$, and (f) $x=10$

dimples at the fracture of the 2.5TiC/FeMnCu alloy.

2.4 Heat treatment for 10TiC/FeMnCu composites

2.4.1 XRD analysis

Fig. 7 shows the XRD patterns of the 10TiC/FeMnCu composite before and after the annealing treatment. After the 10TiC/FeMnCu alloy specimens were annealed under $600\text{ }^\circ\text{C}/4\text{ h}$ and $800\text{ }^\circ\text{C}/4\text{ h}$, the matrix phase structure does not change significantly, but remains as a two-phase face-centred cubic (fcc) structure. In addition to the original face-centred cubic Cu-poor phase and the face-centred cubic Cu-rich phase, metal carbides such as FeC_8 , Fe_2C and Mn_7C_3 are also produced. By comparing the XRD diffraction patterns, it can be found that the change of annealing temperature in this heat treatment process has no significant effect on the phase composition of the 10TiC/FeMnCu composites.

2.4.2 SEM analysis

The SEM images and EDS results of the 10TiC/FeMnCu

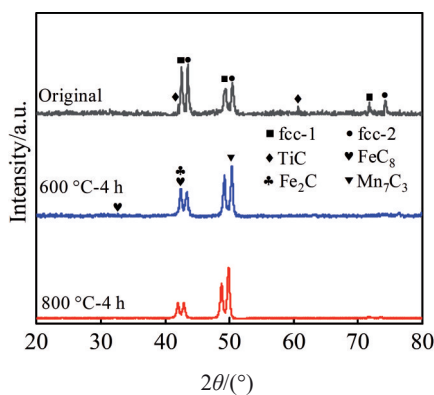


Fig.7 XRD patterns of 10TiC/FeMnCu composites before and after annealing at $600\text{ }^\circ\text{C}$ for 4 h and $800\text{ }^\circ\text{C}$ for 4 h

composites annealed under $600\text{ }^\circ\text{C}/4\text{ h}$ and $800\text{ }^\circ\text{C}/4\text{ h}$ are shown in Fig. 8. It can be seen that the annealed composite still consists of a dark grey Cu-poor matrix phase together with a light grey Cu-rich matrix phase, and the TiC particles are randomly distributed in the matrix and agglomerated. Compared with the case at the annealing temperature of $600\text{ }^\circ\text{C}$, the microstructure of the specimens annealed at $800\text{ }^\circ\text{C}$ is significantly finer and more uniform, and the TiC reinforcement particles are also finer.

2.4.3 Analysis of tensile properties

Fig. 9 shows the stress-strain curves of the specimens before and after the annealing treatment. The ultimate tensile strength of the unannealed specimens and the specimens annealed under $600\text{ }^\circ\text{C}/4\text{ h}$ and $800\text{ }^\circ\text{C}/4\text{ h}$ is 648, 655 and 675 MPa, while their elongation is 32.4%, 13.9% and 11.6%, respectively. From the results, it can be concluded that the 10TiC/FeMnCu alloy shows a small increase in tensile strength but a significant decrease in elongation after annealing under $600\text{ }^\circ\text{C}/4\text{ h}$ and $800\text{ }^\circ\text{C}/4\text{ h}$. It can be attributed to the formation of precipitated phase particles caused by the annealing heat treatment, which affects the tensile strength of the composites. At the same time, the matrix structure of the alloy is refined due to the increase in the annealing temperature, so that the tensile strength appropriately increases. XRD analysis shows that as the heat treatment proceeds, metal carbide particles gradually precipitate in the matrix of the composite, which has the characteristics of high hardness^[30], leading to a reduction in the plasticity of the alloy. As a result of the combined effect of these two factors, the annealed specimens exhibit a small increase in tensile strength and an obvious decrease in elongation at break.

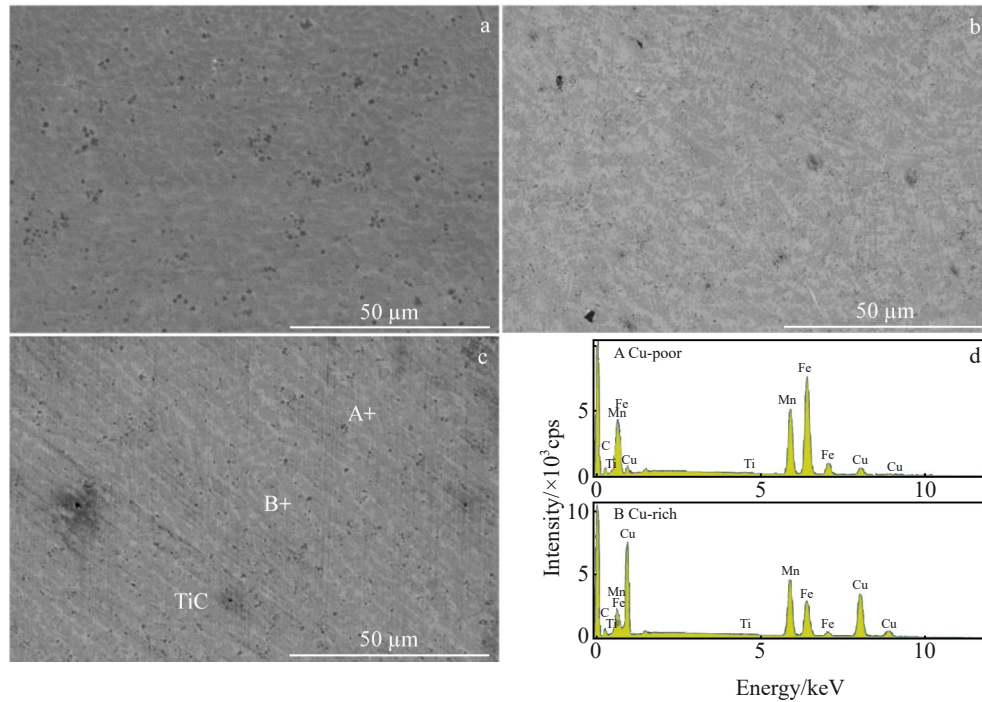


Fig.8 SEM images (a–c) and EDS spectra (d) of 10TiC/FeMnCu composites under different annealing conditions: (a) matrix, (b) 600 °C/4 h, and (c) 800 °C/4 h

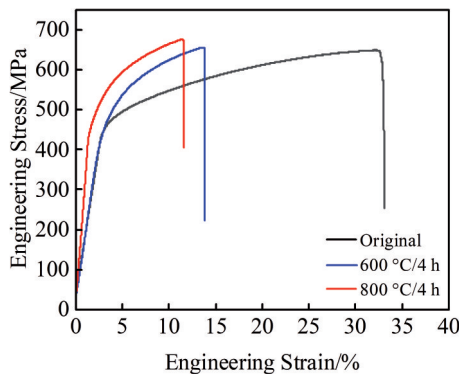


Fig.9 Stress-strain curves of 10TiC/FeMnCu before and after annealing under 600 °C/4 h and 800 °C/4 h

3 Conclusions

1) The x TiC/FeMnCu ($x=0, 2.5, 5, 7.5, 10$, vol%) composites prepared by vacuum induction melting exhibit a biphasic structure, indicating that the addition of TiC-reinforcing particles to the alloy matrix does not change the phase composition of the parent alloy. TiC is randomly distributed in the matrix and gradually agglomerates with increasing x values, and the composite matrix is denser.

2) As the TiC content increases, the tensile strength of the composites increases and the elongation at break first increases and then decreases. 10vol% TiC/FeMnCu alloy has the highest ultimate tensile strength of 648 MPa and 2.5TiC/FeMnCu alloy has the highest elongation at break of 43.9%.

Dimples of varying sizes are present at the tensile fractures, and the morphology all exhibits typical ductile fracture characteristics. The specific strengthening mechanisms present in the x TiC/FeMnCu ($x=2.5, 5, 7.5, 10$, vol%) composites are fine grain strengthening, thermal mismatch strengthening and Orowan strengthening.

3) 10TiC/FeMnCu composites exhibit significant changes in the material structure after annealing under 600 °C/4 h and 800 °C/4 h, accompanied by the precipitation of carbides such as FeC_8 , Fe_2C , Mn_7C_3 . The tensile test of the annealed specimens shows a small increase in tensile strength and a decrease in elongation.

References

- 1 Yeh J W, Chen S K. *Advanced Engineering Materials*[J], 2004, 6(5): 299
- 2 Yeh J W. *Annales de Chimie Science des Matériaux*[J], 2006, 31(6): 633
- 3 Wu Z L, Bei H B, Otto F et al. *Intermetallics*[J], 2014, 46(3): 131
- 4 Jiang J Y, Du J H, Yan J K et al. *Rare Metal Materials and Engineering*[J], 2022, 51(2): 392
- 5 Qiu H, Zhu H G, Zhang J F et al. *Materials Science and Engineering A*[J], 2020, 769(2): 138 514
- 6 Sun X D, Zhu H G, Li J L et al. *Materials Science and Engineering A*[J], 2019, 743: 540
- 7 Zhao C M, Wu H, Zhang J F et al. *Rare Metal Materials and Engineering*[J], 2021, 50(8): 2783
- 8 Łukasz R, Damian K, Anna T et al. *Journal of Alloys and*

- Compounds[J], 2017, 708: 344
- 9 Guo F Y, Yu J K, Xiao J J et al. *Rare Metal Materials and Engineering*[J], 2021, 50(7): 2337
- 10 Gwalani B, Choudhuri D, Soni V et al. *Acta Materialia*[J], 2017, 129: 170
- 11 Lei Z F, Liu X G, Wu Y et al. *Nature*[J], 2018, 563: 546
- 12 Łukasz R, Damian K, Lidia L D. *Intermetallics*[J], 2017, 86: 104
- 13 Senkov O N, Wilks G B, Scott J M et al. *Intermetallics*[J], 2011, 19: 698
- 14 Du X H, Gai Y H, Li W P et al. *Intermetallics*[J], 2022, 146: 107 582
- 15 Xiao Y, Peng X, Fu T. *Vacuum*[J], 2022, 200: 111 017
- 16 Chung D H, Kim W C, Baek S Y et al. *Journal of Alloys and Compounds*[J], 2022, 899: 163 331
- 17 Liao Y C, Chen P S, Tsai P H et al. *Intermetallics*[J], 2022, 143: 107 470
- 18 Gludovatz B, Hohenwarter A, Thurston K V S et al. *Nature Communications*[J], 2016, 7: 10 602
- 19 Ding L, Hilhorst A, Idrissi H et al. *Acta Materialia*[J], 2022, 234: 118 049
- 20 Ahn J E, Kim Y K, Yang S et al. *Journal of Alloys and Compounds*[J], 2022, 918: 165 601
- 21 An N, Sun Y N, Gao L et al. *Journal of Alloys and Compounds*[J], 2022, 914: 165 206
- 22 Liu X W, Laplanche G, Kostka A et al. *Journal of Alloys and Compounds*[J], 2019, 775: 1068
- 23 Moravcik I, Hadraba H, Li L et al. *Scripta Materialia*[J], 2020, 178: 391
- 24 Sathiaraj G D, Skrotzki W N, Pukenas A et al. *Intermetallics*[J], 2018, 101: 87
- 25 Zhang G, Yang X, Zhao Y et al. *Journal of Alloys and Compounds*[J], 2022, 899: 163 221
- 26 Asghari R P, Nguyen N T C, Kim Y et al. *Materials Letters*[J], 2021, 303: 130 503
- 27 Xin B, Zhang A, Han J et al. *Journal of Alloys and Compounds*[J], 2020, 836: 155 273
- 28 Straumal B B, Kucheev Y O, Efron L I et al. *Materials Engineering and Performance*[J], 2021, 21: 667
- 29 Fan Q C, Li B S, Zhang Y. *Materials Science and Engineering A*[J], 2014, 598: 244
- 30 Saha J, Saha R, Bhattacharjee P P. *Intermetallics*[J], 2022, 143: 107 463

TiC增强FeMnCu中熵合金基复合材料的制备及其力学性能

李嘉雯, 刘思聪, 黄思睿, 朱和国

(南京理工大学 材料科学与工程学院, 江苏 南京 210094)

摘要: 采用真空感应熔炼法制备 $x\text{TiC}/\text{FeMnCu}$ ($x=2.5, 5, 7.5, 10, \text{vol}\%$)复合材料, 并对其进行退火热处理。采用X射线衍射仪(XRD)、扫描电镜(SEM)、万能试验机等对所制备合金试样的晶体结构、成分、形貌、力学性能等进行分析。结果表明, $x\text{TiC}/\text{FeMnCu}$ 复合材料呈现出双相面心立方(fcc)结构。随着TiC含量的增加, 复合材料的基体组织得到明显细化, 抗拉强度逐渐增大, 这可能是细晶强化、热错配强化、Orowan强化共同作用的结果。 $10\text{TiC}/\text{FeMnCu}$ 经 $600\text{ }^\circ\text{C}/4\text{ h}$ 、 $800\text{ }^\circ\text{C}/4\text{ h}$ 退火后, 结构没有明显变化, 基体中有碳化物析出, 试样的抗拉强度小幅提升但延伸率略有降低。

关键词: 中熵合金; 真空感应熔炼; TiC增强; 力学性能

作者简介: 李嘉雯, 女, 2000年生, 南京理工大学材料科学与工程学院, 江苏 南京 210094, E-mail: jiawenli0726@163.com